Facies (2007) 53:347–360
DOI 10.1007/s10347-007-0109-1

ORIGINAL ARTICLE

Oligocene cold-seep carbonates from the Carpathians and their inferred relation to gas hydrates

Maciej J. Bojanowski

Received: 13 November 2006 / Accepted: 16 April 2007 / Published online: 30 May 2007

Abstract The Krosno Formation of the Outer Carpathians is composed of synorogenic deposits laid down in the Silesian foredeep basin in front of an accretionary prism. The Oligocene shales of the Krosno Formation from Świątkowa Wielka (the Polish part of the Outer Carpathians) contain numerous authigenic carbonate rocks: concretions, a laminated limestone bed, and a carbonate build-up consisting of intraformational breccia. The application of stable carbon isotope analysis revealed that the formation of these carbonates was induced by methane oxidation. The presence of fossilized giant *Beggiatoa*-like filaments and large quantities of framboidal pyrite indicate that methane oxidation was microbially driven and coupled with sulfate reduction. A model of origin of these cold-seep carbonates in relation to hydrocarbon seepage is herein presented. Characteristic druses with clast-like appearance are thought to inherit their outlines from former clasts of gas hydrate that had been present within the build-up. It is proposed that thick gas hydrate deposits existed in the southern part of the Silesian basin at that time. This theory is consistent with regional, geotectonic, and palaeobathymetric data and provides a ready explanation of the major phenomena that have been recorded in the Krosno Formation.

Keywords Hydrocarbon-seeps · Authigenic carbonates · Bacteria · Gas hydrates · Oligocene · Outer Carpathians

M. J. Bojanowski (✉)
Instytut Geochemii, Mineralogii i Petrologii,
Wydział Geologii, Uniwersytet Warszawski,
Al. Żwirki i Wigury 93, 02-089 Warszawa, Poland
e-mail: mcbojan@uw.edu.pl

Introduction

Cold-seep carbonates form as by-products of chemosynthetically driven hydrocarbon oxidation in marine sediments. Migration of source fluids charged with hydrocarbons is often related to convergent plate margins and accretionary prisms (Ritger et al. 1987; Sakai et al. 1992; Von Rad et al. 1996; Bohrmann et al. 1998; Suess et al. 1999). The Outer Carpathians are a Miocene thrust-and-fold orogenic belt composed of a thick succession (mainly turbiditic) that dates from Jurassic to Miocene (Poprawa et al. 2002; Oszczypko 2004). The youngest flysch deposits, the Krosno Formation, are a syntectonic facies deposited in front of an accretionary prism (Picha and Stranik 1999; Poprawa et al. 2002; Oszczypko 2004). Large submarine slumps, soft-sediment deformations, and fluidization structures are numerous in this formation (e.g. Książkiewicz 1949; Dżułyński and Radomski 1956; Książkiewicz 1958). It also hosts various carbonate rocks, mostly as exotics (e.g. Ślączka 1961; Ślączka and Wieser 1962; Mochnacka and Tokarski 1972; Burtan et al. 1984).

Carbonate rocks from the Krosno Formation near Świątkowa Wielka have also been interpreted as exotics (e.g. Kozikowski 1956; Koszarski 1985; Mastella and Rubinkiewicz 1998). This paper presents the results of detailed petrographic reexamination and the application of stable carbon isotope analysis to these rocks. It shows that they are authigenic and that anaerobic oxidation of methane induced their formation. Migration of methane-bearing fluids was related to the formation of an accretionary prism and probably also to the decomposition of gas hydrate deposits. The occurrence of gas hydrates is inferred not only from theoretical evaluation of gas hydrate stability in the Silesian basin, but also from petrographic observations. Fossilized *Beggiatoa*-like filaments found within the

authigenic carbonates are the direct proof of microbial activity related with the seepage.

Because such authigenic seep carbonates from foredeep turbidite basins are symptoms of the advancing deformational front, they are a crucial element in the reconstruction of the major tectono-sedimentary events of the orogenesis. They are the evidence of fluid expulsion and hydrocarbon emanation phenomena that are otherwise not preserved in geological record. This work contributes to the knowledge concerning hydrocarbon palaeoseeps (see review by Campbell 2006) and introduces valuable information to the understanding of the final stages of the Carpathian basin development.

Regional setting

The eastern part of the Polish Outer Carpathians is composed of six main nappes (from south to north): Magura, Grybów, Dukla, Silesian, Subsilesian, and Skole nappes (Fig. 1). Magura, the uppermost nappe in the Outer Carpathians, is thrust over the Grybów, the Dukla and the Silesian nappes. The Grybów nappe is almost entirely covered by the Magura nappe and emerges only within tectonic windows (Cieszkowski et al. 1985). The sedimentary infilling of the Polish Outer Carpathians was deposited in three independent basins (from south to north): Magura, Silesian and Skole basins (Pescatore and Ślączka 1984; Oszczypko 2004). The Grybów and the Dukla nappes exhibit transitional litho-facies that link the Magura and the Silesian basins (Oszczypko-Clowes and Oszczypko 2004). The Late Eocene–Oligocene rocks of the Grybów and the Dukla nappes reveal lithological similarities with the Silesian nappe (Unrug 1968; Cieszkowski et al. 1985; Oszczypko 2004) and were deposited in the southern marginal part of the Silesian basin (the Dukla subbasin; Jucha and Kotlarczyk 1961; Unrug 1968; Cieszkowski et al. 1985).

The cold-seep carbonates that are the subject of this paper occur in the Oligocene Krosno Formation in the Grybów nappe that crops out from beneath the Magura nappe within the Świątkowa Wielka tectonic window. Świątkowa Wielka is situated in the Beskid Mały mountains, about 5 km west from Krempna (Fig. 1). The Krosno Formation at this location comprises a series of turbiditic/hemipelagic mudstones that were deposited in the southern marginal part of the Silesian basin (in the Dukla subbasin) during the formation of an accretionary prism that was approaching from the south from the Magura basin (Picha and Stranik 1999; Poprawa et al. 2002; Oszczypko 2004). The Magura nappe began to develop in the Late Oligocene when it was thrust over the Dukla subbasin (Pescatore and Ślączka 1984; Poprawa et al. 2002; Oszczypko-Clowes and Oszczypko 2004). As a result of the subsequent northward migration of the orogenic front, nappes were thrust over each other in the Silesian and the Skole basins in the Early Miocene (Pescatore and Ślączka 1984; Poprawa et al. 2002; Oszczypko 2004).

Methods

Standard petrographic microscopy was performed on thin sections. Some thin sections were stained with alizarin red

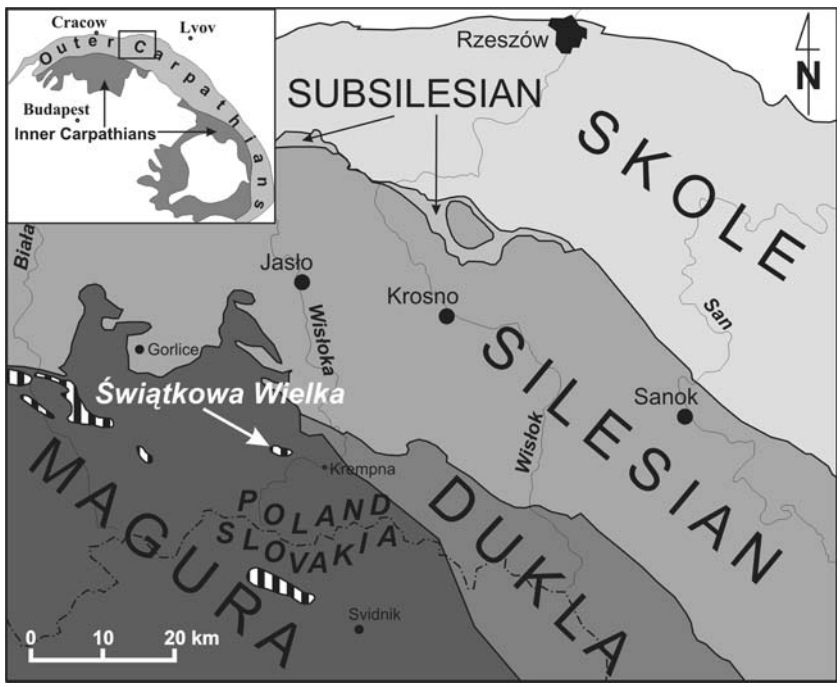

Fig. 1 General map of tectonic units of the eastern part of the Polish Outer Carpathians. The nappes are thrust in the NNE direction. The Grybów nappe (*stripes*) is covered by the Magura nappe and emerges only within tectonic windows. Seep carbonates occur in the Grybów unit which crops out in the Świątkowa Wielka tectonic window (*arrow*)

and Feigl's solution according to the procedure described by Friedman (1959). Because the examined rocks are very fine-grained, detailed observations and analysis of mineral and elemental composition were performed using electron microscopy. Uncovered thin sections, polished and powdered with carbon, were examined using a WDS Cameca SX-100 microprobe (Faculty of Geology, Warsaw University, Poland). Observations were carried out using backscattered electron imaging. Operating conditions: 15 kV accelerating potential, 10–20 nA beam current. Rock chips coated with gold were examined using a JEOL JSM-6380LA scanning electron microscope equipped with EDS analyzer (Scanning Electron Microscope and Microanalysis Laboratory at Faculty of Geology, Warsaw University, Poland). Cathodoluminoscopy was conducted on uncovered, polished thin sections using the Premier American Technologies cold cathode-Luminoscop ELM-3R (Geological Bureau GEONAFTA, Warsaw, Poland). Operating conditions: 5–20 kV beam energy, 1 mA beam current, 20–80 mT vacuum. For the fluid inclusion studies double-polished sections 0.5 mm thick were glued on 1-mm-thick glass plates with epoxy resistant to high temperatures. The analysis was conducted according to the routine heating/freezing microscopic method (Roedder 1984) using the Fluid Co., Inc. (USA) microscope stage. The fluid inclusion studies were performed by Prof. Andrzej Kozłowski (Faculty of Geology, Warsaw University, Poland). Rock-Eval pyrolysis was carried out on powdered samples (100 mg each) using Rock-Eval 6 apparatus (Oil and Gas Institute, Kraków, Poland). This technique allows continuous detection of CO and CO_2 released during pyrolysis and oxidation. S_1, S_2, S_3 and T_{max} values were recorded during programmed heating (from 100 up to 650°C) of the pyrolysis oven in nitrogen atmosphere. Then, the sample was placed in the oxidation oven where it was combusted in air at 850°C to give S_4 value. Replicate analyses of the standard used (IFP no. 16,000) agreed to within ±1°C for T_{max}, ±5% for TOC and ±10% for S_1, S_2 and S_3 of a mean value.

Samples for stable carbon isotope analysis were small chips (about 0.1–0.5 cm^3) obtained with the highest possible precision by using a very small chisel. Shale samples were taken from individual beds (less than 10 mm thick). About 5-mm-thick slabs were cut from the carbonates and the samples were taken avoiding inclusion of material which had been in contact with the shales. Stable carbon isotope measurements were performed on powdered bulk samples reacted with 100% phosphoric acid (density 1.9, Wachter and Hayes 1985) at 75°C using a Kiel III online carbonate preparation line connected to a ThermoFinnigan 252 mass spectrometer (University of Erlangen, Germany). All values are reported in per mil relative to V-PDB by assigning a $\delta^{13}C$ value of 1.95‰ to NBS19. Reproducibility (1σ) was verified by replicate analyses of laboratory standards and is better than ±0.02‰.

Results

Petrography of the host sediments

The Krosno Formation is represented by a sequence of dark-grey calcareous mudstone about 100 m thick (the so-called "Krosno shales"). The mudstone is composed of two kinds of beds of different origin: turbiditic and hemipelagic. A wide variety of soft-sediment deformations (e.g. slump folds and mud breccia) is encountered in the mudstone. These structures reveal that the hemipelagic beds were deformed plastically (were semi-consolidated), whereas more coarse-grained turbidite material was fluidized during deformation.

Petrography of the authigenic carbonates

The Krosno shales host various carbonate rocks (Fig. 2). A lenticular mound-shaped carbonate body (10 m high and 50 m wide) composed of carbonate intraformational breccia thins gradually into a layer of laminated limestone. The thickness of the limestone bed decreases away from the carbonate build-up from 1 to 20 cm. Boulders of the carbonate breccia appear on the sides of the build-up above the limestone layer, forming a kind of a talus. Numerous calcite concretions ranging from a millimeter (Fig. 3a) to a few decimeters in lateral dimension are dispersed below and above the limestone bed.

All the carbonate rocks are composed mainly of microcrystalline calcite (Fig. 3a). The remaining material constitutes only a minor addition and is the same as in the host Krosno shales: siliceous (quartz, clay minerals, micas, feldspars), carbonate (calcite foraminifers and coccoliths, detrital calcite and authigenic dolomite), framboidal pyrite, and organic matter (Fig. 3a). However, the content of organic matter and pyrite is sometimes noticeably increased in the carbonates relative to the mudstone. Pyrite framboids are authigenic and their textural relationship with authigenic calcite indicates that calcite precipitation was concurrent or preceded by pyrite formation.

Thanks to early-diagenetic, precompactional cementation (Bojanowski 2001), the original texture of the sediments has been "frozen" in the authigenic carbonates. The limestone bed (Fig. 3b) and some of the concretions (Fig. 3c) inherited the original lamination of the sediments. Most of them precipitated within undisturbed deposits and preserved parallel lamination, but early-diagenetic deformations also appear. Synsedimentary folds are found within the limestone bed (Fig. 3b). A few concretions enclosed already brecciated sediments (Fig. 3d). Burrows and septarian cracks often cut the lamination in the concretions (Fig. 3c). Some of the septarian cracks are filled with yellow blocky calcite (Fig. 3c) that constitutes the last generation of calcite cements. This calcite is rich in fluid

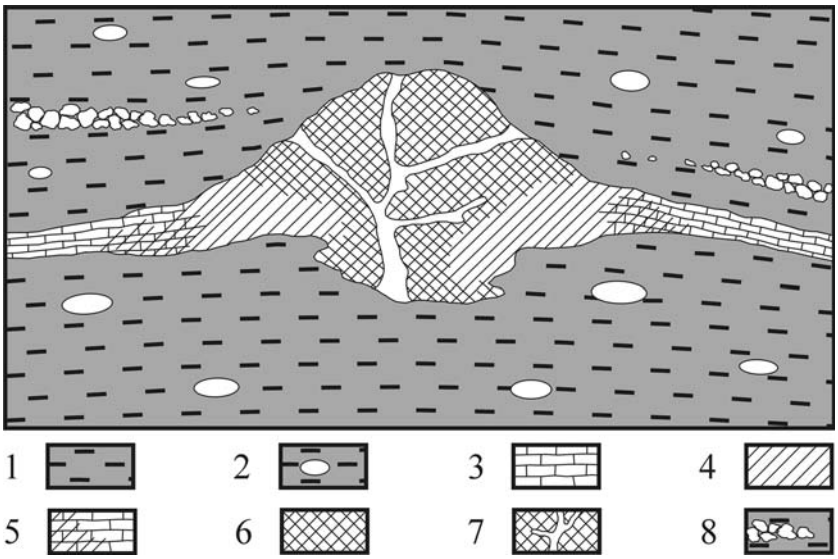

Fig. 2 A schematic sketch of the distribution of the seep carbonates examined showing the internal structure of the carbonate build-up (not to scale, vertical dimension of the sketch corresponds to approximately 20 m). (*1*) Mudstone; (*2*) Mudstone with concretions; (*3*) Laminated limestone bed; (*4*) Monomictic breccia; (*5*) Laminated limestone intensively fractured; (*6*) Polymictic breccia; (*7*) Conduit zones in the polymictic breccia; (*8*) Mudstone with debris of the carbonate breccia from the build-up

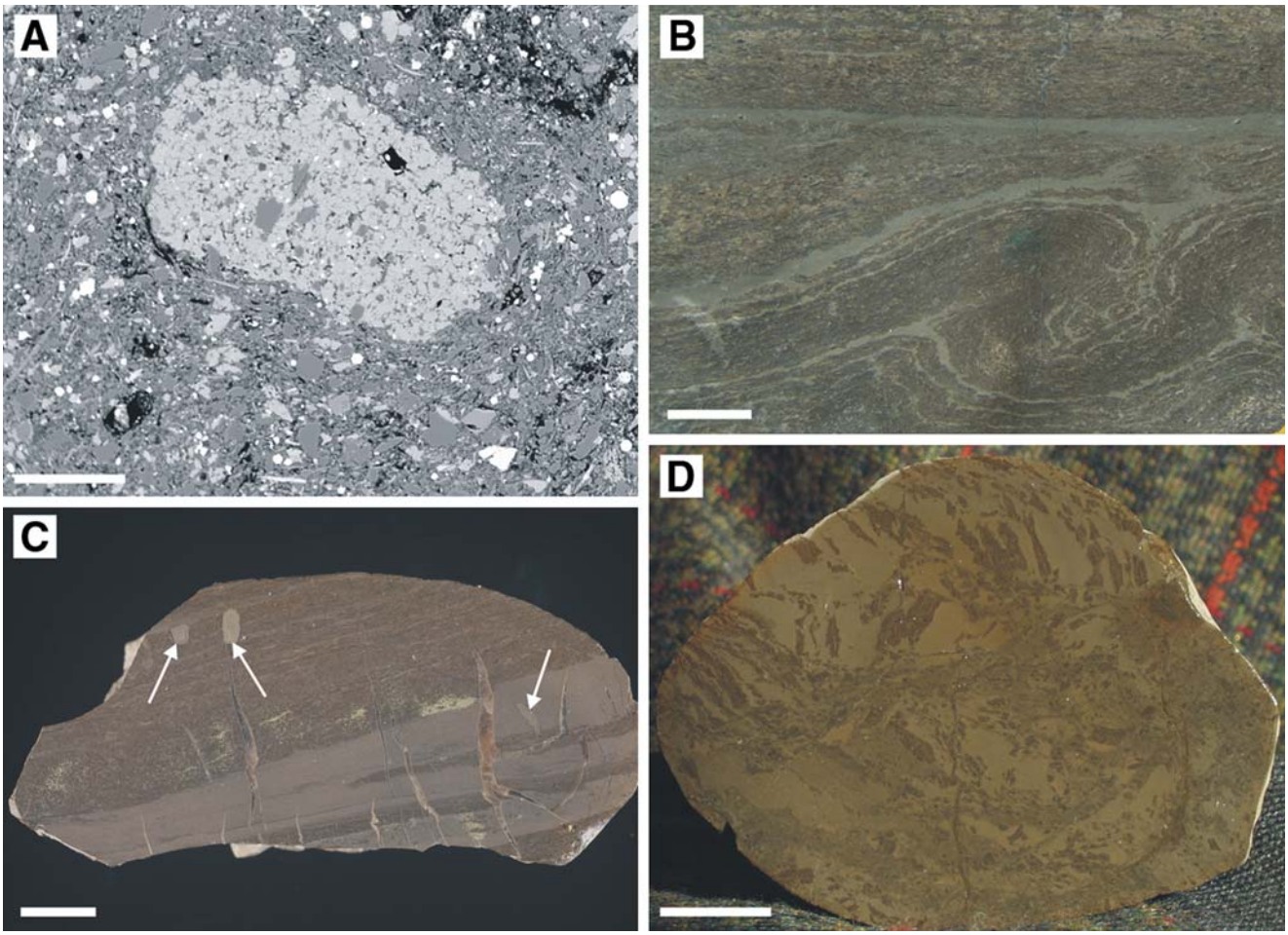

Fig. 3 Images of the concretions and the laminated limestone bed: **a** back-scattered image of a microconcretion enclosed within the host mudstone. Microcrystalline authigenic calcite (*light grey*) is the dominant constituent of the microconcretion. Sediment particles, mainly quartz and micas (*dark grey*), but also calcite (*light grey*) and authigenic framboidal pyrite (*white*), occur in the microconcretion and the host rock. Scale bar: 0.1 mm. **b** The laminated limestone with synsedimentary folds. Scale bar: 10 mm. **c** Cross section of the laminated concretion with burrows (*arrows*) and septarian cracks filled with yellow blocky calcite. Scale bar: 20 mm. **d** Cross section of the concretion, which cemented brecciated mudstone. Scale bar: 20 mm

inclusions, which formed at temperatures below 40°C. Some of the inclusions are filled with gas: carbon dioxide and/or methane.

The limestone bed is pervaded by a dense, irregular network of carbonate-filled veins in the vicinity of the carbonate build-up. The degree of fragmentation increases so that the fractured limestone changes gradually to a monomictic intraformational breccia on the flanks of the build-up (Fig. 2). Clasts of the laminated limestone in the monomictic breccia are only slightly dislocated and many of them exhibit dark rims (Fig. 4a). The space between the clasts is filled mainly with microcrystalline authigenic calcite but also with detrital and biogenic material.

Towards the center of the build-up, the monomictic breccia is gradually replaced by a polymictic breccia, which makes up most of the carbonate structure (Fig. 2). The clasts in the polymictic breccia are mostly carbonate and include fragments of the laminated limestone and the monomictic breccia (Fig. 4b). Clasts of the Krosno shales appear only in the conduit zones (Fig. 4c), which occur in the center of the build-up (Fig. 2). The clasts are chaotically dispersed and exhibit various morphologies that indicate plastic, brittle and fluidal deformations.

Similar to the monomictic breccia, the carbonate clasts in the polymictic breccia often have dark rims (Fig. 4d), which are bright yellow under CL (Fig. 4e). Microprobe analysis of both breccia types revealed that these coatings are composed of calcite cement and bitumen (Fig. 4f). Unlike the clasts and the space between them, the coatings are barren of detrital particles; they consist exclusively of authigenic calcite and bitumen (Fig. 4f). They are usually less than 0.2 mm thick and clearly represent organic-rich calcite overgrowths of the clasts.

The space between the clasts in the polymictic breccia has a similar composition and texture to that in the monomictic breccia. However, irregular vuggy and stromatactis-like structures also appear. At places, the space between the clasts is full of dark druses which show a characteristic fabric: they resemble clasts, because they have angular shapes and are closely spaced (Fig. 5). The walls of the druses are lined with fringes of calcite and they do not contain any sediment particles (Fig. 6).

Most of the druses are completely filled with bitumen and calcite (Figs. 5, 6). Apart from the fringe cement they contain rod-shaped calcite crystals randomly oriented in the center (Fig. 6). The rod-shaped crystals are sometimes curved and small pyrite aggregates (a few μm in diameter) are commonly found within them (Fig. 6b). Under CL the fringe cement reveals lamination along the walls of the druses (Fig. 6e–f), while the rod-shaped crystals are concentrically zoned (Fig. 6f).

Some druses, however, may still be unfilled in the center (Figs. 5, 6c, e, 7a) and occasionally large filaments (3–20 μm wide, up to 2 mm long) are found there (Fig. 7). These filaments are hollow (Fig. 7b), thread-like and unbranched with rounded tips (Fig. 7c). The filaments are rooted within aggregates of the fringe cement that lines the cavity wall (Fig. 7d). An EDS analyzer revealed that the filaments are composed of $CaCO_3$ and that original cell material has not been preserved. Bitumen (most likely microbially oxidized crude oil) covers the inner surface of the void (Fig. 7d) and the calcified filaments. (Fig. 7c–d). In some places, very small (several microns) calcite crystals appear on the bitumen coatings (Fig. 7c–d).

Types of organic matter

The Rock-Eval pyrolysis revealed that the rocks contain different types of organic matter (OM) determined on the basis of HI/T_{max} ratio. The proportion of marine to terrestrial OM increases from the Krosno shales (terrestrial type IIIb OM) through the concretions (mainly terrestrial type IIIa OM) to the laminated limestone bed and the clast-like druses from the polymictic breccia (mixed type IIb OM).

Carbon stable isotopic composition

The Krosno shales show $\delta^{13}C$ values between −4 and 0‰ (19 samples) (Fig. 8). All of the carbonate rocks are strongly depleted in ^{13}C and exhibit $\delta^{13}C$ values between −39 and −16‰ (42 samples; Fig. 8): the concretions from −39 to −16‰; the limestone bed from −37 to −19‰; the breccia (samples from the clasts, the spaces between them and from the druses) from −30 to −24‰.

Discussion

Sources of carbonate carbon

The $\delta^{13}C$ values in all the carbonate rocks examined are average values of the entire carbonate fraction, which encompasses authigenic, biogenic and detrital material. Biogenic and detrital carbonates have $\delta^{13}C$ values around 0‰ just as the Krosno shale samples (Fig. 8). Therefore, the authigenic carbonates are probably even more ^{13}C-depleted than is suggested by the $\delta^{13}C$ values (Fig. 8). All of the carbonate rocks reach −30‰ or lower $\delta^{13}C$ values, which indicates that the precipitation of calcite was induced by hydrocarbon oxidation (Whiticar and Faber 1986). The presence of gaseous inclusions filled with carbon dioxide and methane within the last generation of calcite cements reveal that both gases coexisted in the pore waters. It is not possible to determine unequivocally the origin of the hydrocarbons, because the isotopic signature may be equally

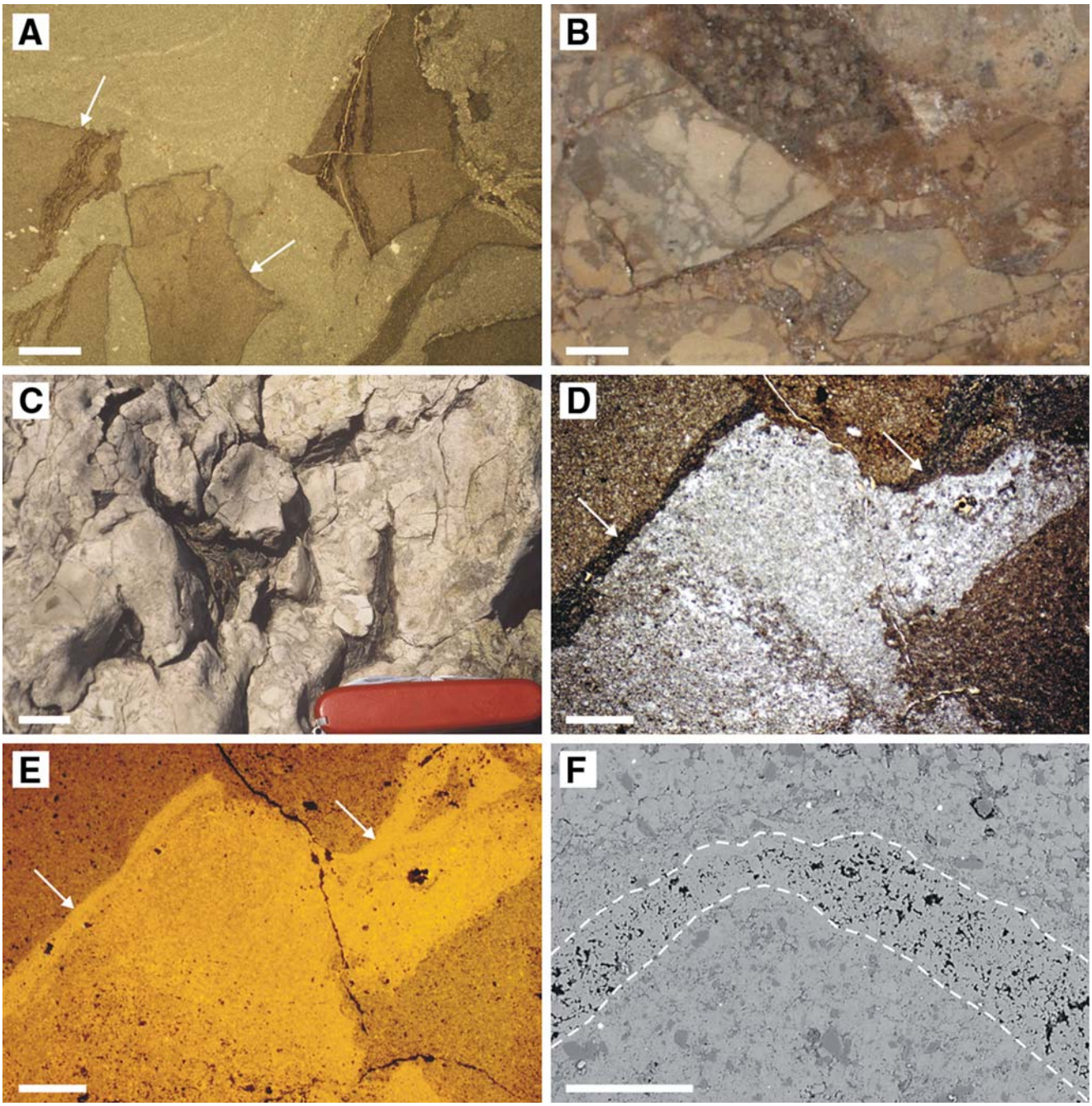

Fig. 4 Images of the carbonate breccia. **a** Thin section (plane polarized light) of the monomictic breccia with the clasts of the laminated limestone coated with dark band (*arrows*). Some clasts fit to each other like a puzzle (*left*). Scale bar: 2 mm. **b** Cross section of the polymictic breccia with the clasts of the monomictic breccia. Scale bar: 10 mm. **c** The polymictic breccia from the conduit zone with the clasts of the Krosno shale. Scale bar: 20 mm. **d** Thin section (nicols crossed) of the monomictic breccia with the brown clast on the left coated with dark band (*arrows*). The space between the clasts is *light grey* (*in the center*). Scale bar: 1 mm. **e** CL image of **d**. Note the bright yellow luminescence of the bands (*arrows*) when compared to the darker luminescence of the clasts and the space between them, which is caused by the presence of sediment particles in the latter. Scale bar: 1 mm. **f** Back-scattered image of the polymictic breccia. Authigenic calcite (*light grey*) is the dominant constituent. Sediment particles, mainly quartz and micas (*dark grey*), and framboidal pyrite (*white*) occur in the clast (*bottom*) and the space between the clasts (*top*). The clast is overgrown by a thin band of calcite cement (between the *dashed lines*), which is a pure precipitate (barren of sediment particles) with bitumen (*black*) filling large pore spaces. Scale bar: 0.1 mm

indicative of biogenic and thermogenic genesis of the source hydrocarbons (see Wellsbury and Parkes 2000). Hydrocarbon oxidation was probably coupled with sulfate reduction, since framboidal pyrite formed before and/or simultaneously with calcite precipitation, and since oxidation of methane in oxic conditions would drive carbonate

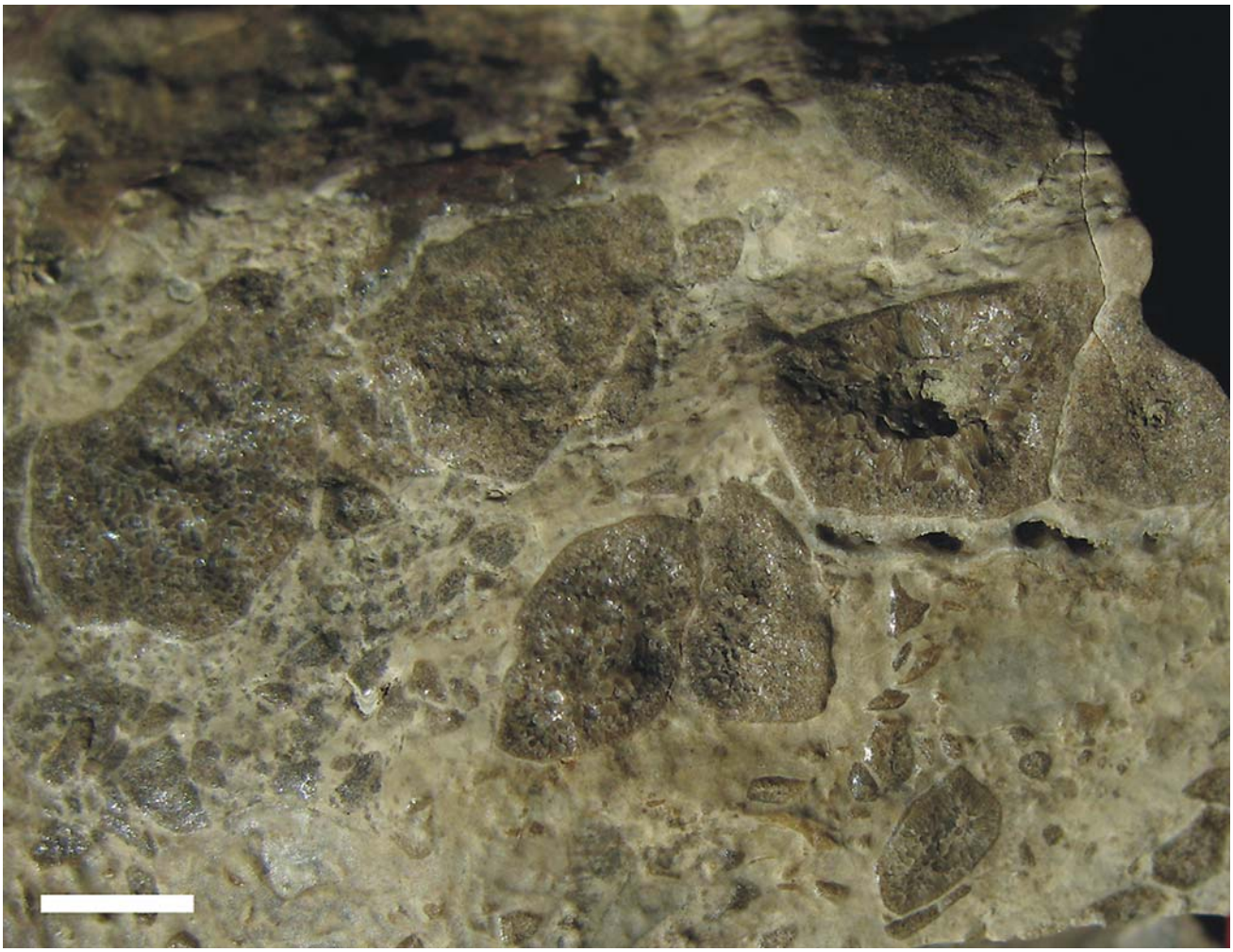

Fig. 5 Characteristic clast-like druses from the polymictic breccia. Note their angular outlines and that some of them are closely spaced and fitting together like a puzzle. Fringe calcite cement lines the cavity walls. The brown color of the infillings comes from bitumen. One of the druses (*on the right*) is still hollow in the center. Scale bar: 5 mm

dissolution rather than precipitation (Cranston and Buckley 1990; Jahnke et al. 1994).

Origin of the carbonates

Minor diffuse seepage of methane led to the formation of the concretions (Fig. 3a–d) that are dispersed in the host rock (Fig. 2). A more intensive supply of methane induced more extensive cementation that resulted in the formation of the limestone bed (Fig. 3b). The limestone bed started to act as a permeability barrier and the ascending fluids charged with methane were trapped beneath it. The resultant overpressure in pore waters caused fluidization and soft-sediment deformations in the mudstone (Fig. 3d). The subsequent flow of fluids became more focused and probably followed a tectonic feature (a fault or an initial thrust of the arising accretionary prism). Rapid fluid rise along such a discontinuity greatly increased the overpressure. At some point the fluids were abruptly released which caused brecciation of the limestone bed.

Monomictic breccia (Fig. 4a) was formed in situ in places where the abrupt discharge of the fluids occurred rarely, most probably only once. Polymictic breccia (Fig. 4b, c) developed where the extrusions were much more intensive and frequent. The fact that the clasts of the monomictic breccia occur in the polymictic breccia (Fig. 4b) proves that brecciation happened repeatedly and interchangeably with cementation. The clasts (both the mudstone and the seep carbonates) were deformed, chaotically mixed and transported upwards, where they were cemented by methane-induced carbonate precipitation. This recycling process gradually led to the development of the carbonate build-up with its distinctive internal structure (Fig. 2).

The carbonate build-up was slightly elevated above the seafloor and breccia blocks slid down to form a kind of a

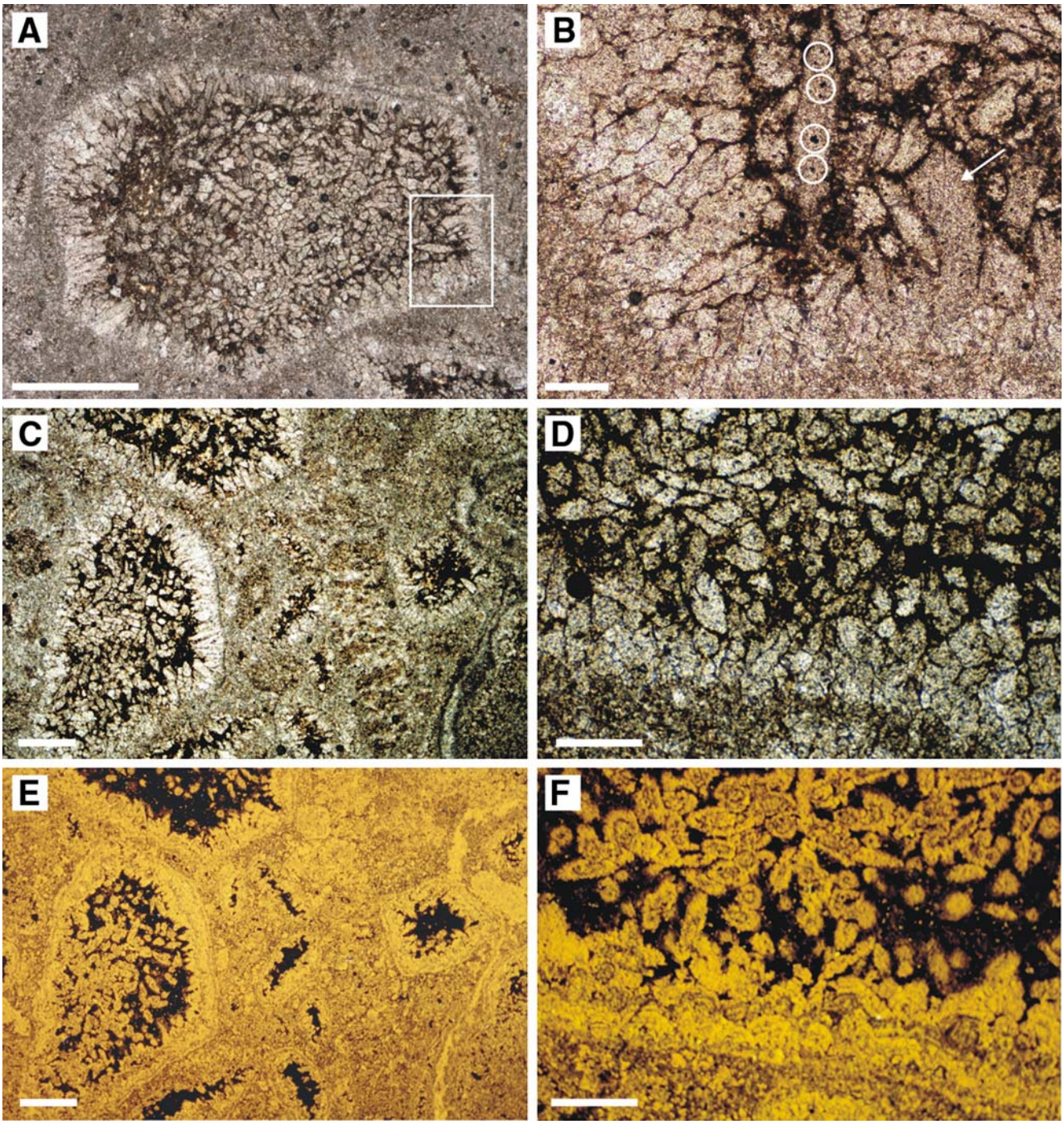

Fig. 6 Thin sections of the clast-like druses from the polymictic breccia. **a** Plane polarized light. The druse exhibits clast-like outline. It is bordered by fringes of calcite cement and contains bitumen and rod-shaped crystals *in the center*. Scale bar: 1 mm. Detail of the druse (*in the rectangle*) is shown in (**b**). **b** Plane polarized light. Detail of (**a**). Note the rod-shaped calcite containing six pyrite globules (*in circles*) and the curved calcite crystal (*arrow*). Scale bar: 0.1 mm. **c** Plane polarized light. The druses are bordered by fringes of calcite cement. Some druses are void and contain only bitumen (the *small one on the right*), but usually rod-shaped crystals appear there (in the *large one on the left*). Scale bar: 2 mm. **d** Plane polarized light. Close-up view of the druse. Fringe cement *at the bottom*, rod-shaped crystals *at the top* of the image. Scale bar: 1 mm. **e** CL image of (**c**). The angular clast-like outlines of the druses are evident. The fringe cement exhibits lamination along the cavity wall. Note the bright yellow luminescence of the infilling when compared to the darker luminescence of the space between the druses which is caused by the presence of sediment particles in the latter. Scale bar: 2 mm. **f** CL image of (**d**). The lamination of the fringe calcite cement along the cavity walls can be observed at the bottom of the image. The *rod-shaped* crystals at the top of the image show concentric zoning. Scale bar: 1 mm

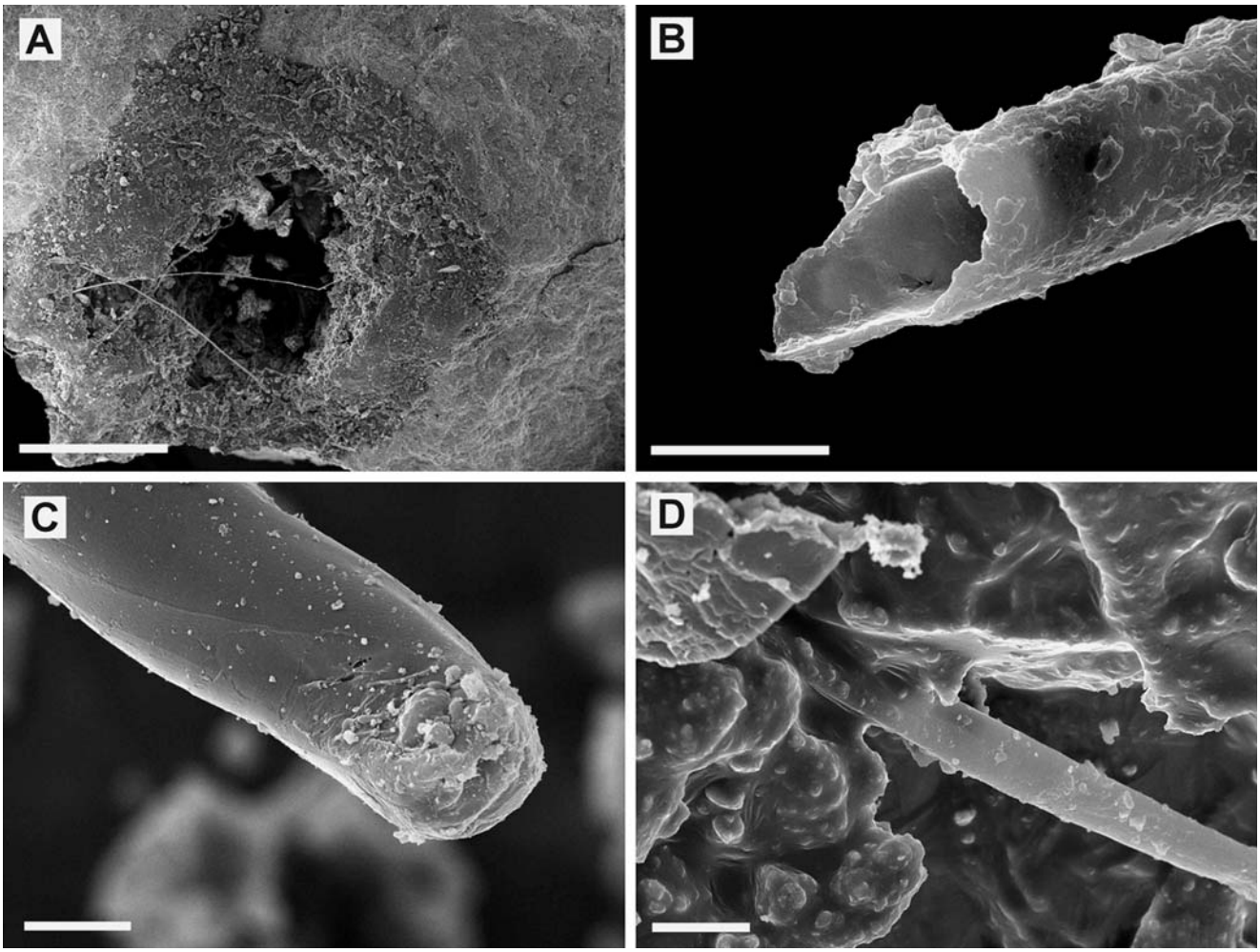

Fig. 7 SEM images of the fossilized filaments from the polymictic breccia. **a** Entire druse with the largest filaments visible. Some of them are even detectable with unaided eye. Scale bar: 1 mm. **b** Hollow interior of a broken filament. Scale bar: 10 μm. **c** Rounded tip of a filament coated with bitumen and very small calcite crystals. Scale bar: 10 μm. **d** A filament rooted within the fringe calcite cement. The crystals and the filament are coated with bitumen. Scale bar: 20 μm

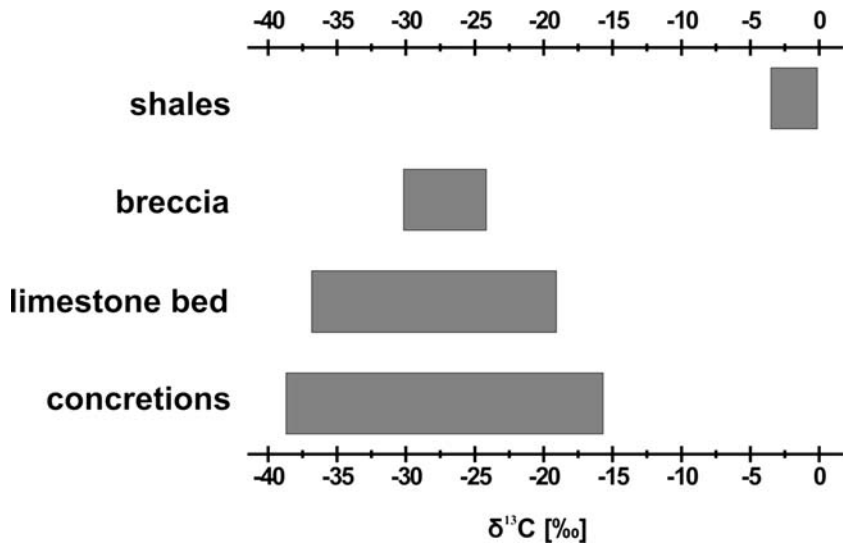

Fig. 8 Ranges of the $\delta^{13}C$ values of the host Krosno shales and the three types of authigenic carbonate rocks: the calcite concretions, the laminated limestone bed and the carbonate breccia

talus (Fig. 2). However, it is not clear whether it grew actively into the seawater and can be termed "chemoherm" sensu Teichert et al. (2005) or was exhumed due to sediment winnowing later on. It lacks any chemotrophic macrofauna typical for chemoherm carbonates. This fact may suggest subsurface growth that prevented macrofauna from colonization. However, the presence of macroorganisms around cold seeps can be limited by depth (Sassen et al. 1993), oxygen availability (Von Rad et al. 1996; Sassen et al. 2004), or other colonization barriers and there are reports of chemoherms barren of macrofauna, containing only microbial mats (Sassen et al. 1993; Von Rad et al. 1996). Therefore, above-seafloor precipitation of the carbonate build-up is uncertain, although it cannot be excluded.

Fossil evidence of seep-related microbial activity

The mixed type of OM from the laminated limestone bed and the clast-like druses from the polymictic breccia in comparison to the terrestrial type of OM from the host mudstone implies that the formation of the authigenic carbonates was accompanied by the flourishing of marine microorganisms. The addition of marine-type OM generated by decomposition of such biota to the "normal" terrestrial-type OM of the sediments resulted in the overall mixed type of OM in the seep carbonates.

Further evidence of microbial activity comes from petrographic observations. Thin bands of calcite cement and bitumen that cover many clasts in the breccia (Fig. 4a, d–f) are obviously organic-rich precipitates. Their composition, structure, placement and thickness match the typical features of biofilms (see Riding 2002) and are thought to represent mineralized biofilms (see Peckmann et al. 1999). They probably formed due to bacterially induced calcification.

A more direct indication of microbial activity are filaments which have been preserved within the druses of the polymictic breccia (Fig. 7). The shape and size of the hollow filaments (3–20 μm wide, up to 2 mm long) match *Beggiatoa*, vacuolate sulfide-oxidizing bacteria (Larkin and Henk 1989; Larkin et al. 1994). The filaments do not exhibit tapered ends and do not form cords, features characteristic of other sulfur bacteria such as *Thioploca* (Nelson et al. 1989; Jørgensen and Gallardo 1999). Therefore, on the basis of morphologic analogy to *Beggiatoa*, the fossilized filaments will be referred to as *Beggiatoa*-like filaments.

Beggiatoa are commonly found associated with modern hydrocarbon seeps (Sassen et al. 1993; Larkin et al. 1994; Joye et al. 2004; Sassen et al. 2004; Teichert et al. 2005) and their filaments are sometimes preserved in ancient seep carbonates (Cavagna et al. 1999; Peckmann et al. 2004; Barbieri and Cavalazzi 2005). They are capable of oxidizing sulfide provided by anaerobic oxidation of methane (Larkin et al. 1994; Teichert et al. 2005), a process mediated by methane-consuming consortia of archea and sulfate-reducing bacteria (Boetius et al. 2000; Orphan et al. 2001). They are also observed to live directly on the surface of decomposing gas hydrate (Sassen et al. 2004).

The very negative $\delta^{13}C$ values (as low as 30 ‰) of the druse fillings indicate that the calcite precipitation was induced by oxidation of methane. The *Beggiatoa*-like filaments examined are rooted within the fringe calcite cement (Fig. 7d), which proves that they were fossilized before or during methane-related precipitation of the fringe cement. Thus, the fossilized filaments provide direct evidence of ancient microbial activity related to hydrocarbon seepage that induced carbonate precipitation.

The filaments examined are exceptionally well preserved (Fig. 7), which indicates their very early post-mortem fossilization. Most likely, the calcification occurred already during decomposition of the original cell material and was related with oxidation of methane. This methane-related carbonate precipitation had the potential to preserve the fragile structure of *Beggiatoa*-like bacteria, which is an exceptional situation (see Peckmann et al. 2004; Barbieri and Cavalazzi 2005).

Most of the druses are entirely filled and in the center they contain rod-shaped calcite crystals (Fig. 6), which show concentric fabric in CL (Fig. 6f). It is possible that some of the rod-shaped crystals are also *Beggiatoa*-like filaments, but observed in two dimensions in the thin section. This would explain their shape (Fig. 6), tubular zonation (Fig. 6f), and the occurrence of pyrite within them (Fig. 6b). These pyrites are probably pyritized elemental sulfur globules, which are stored by sulfide-oxidizing bacteria, like *Beggiatoa*, within their cells (Jørgensen and Revsbech 1983; Nelson et al. 1989; Peckmann et al. 2004).

Possible relation to gas hydrates

Conditions for gas hydrate formation

The possible occurrence of gas-hydrate deposits in the Oligocene Silesian basin is evaluated (Fig. 9) according to the phase boundary data for the oceanic gas-hydrate from Dillon and Max (2000) and the following assumptions. The depth of the Silesian basin during the sedimentation of the Krosno Formation is not precisely determined, but there is a common agreement that it was in the lower part of the upper bathyal zone or slightly deeper, i.e, between 400 and 1,000 m (Książkiewicz 1975; Olszewska 1984; Poprawa et al. 2002). Since the Silesian basin was developed upon thinned continental crust (Książkiewicz 1977; Pescatore and Ślączka 1984;

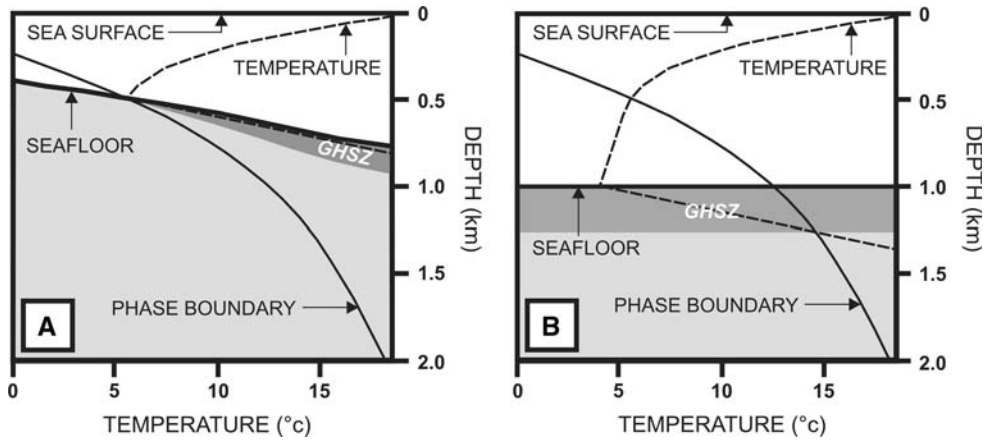

Fig. 9 Evaluation of the gas hydrate stability in the Silesian basin in Oligocene. In the schematic temperature vs. depth diagrams the stability field of gas hydrate in seawater extends below the solid curve (phase boundary). Gas hydrate would be stable below the seafloor where the temperature curve (*dashed line*) goes below the phase boundary. The inclination of the temperature curve below the seafloor is dependent on the geothermal gradient. Given the assumptions described in the discussion on conditions for gas hydrate formation, two temperature vs. depth diagrams were constructed: **a** shows that gas hydrates could have existed below the seafloor where the depth of the basin exceeded 500 m, while **b** illustrates the conditions of gas hydrate stability in a 1,000-m-deep basin

Nemčok et al. 2001), a slightly increased geothermal gradient is assumed (40°C/km). The Northern Carpathian basins in the Oligocene experienced a rather cool climate (Van Couvering et al. 1981), so typical North Atlantic Ocean thermal conditions were chosen (Dillon and Max 2000). The resultant diagram (Fig. 9) shows that gas hydrate could be formed in the Silesian basin from about 500 m depth and would attain maximum thickness of about 250 m in the deepest parts of the basin at 1,000 m depth.

The formation of gas hydrates in the Silesian basin required an efficient source of hydrocarbons. The Menilite Formation that underlies the Krosno Formation has a very good source-rock potential in the entire Carpathian overthrust belt (Köster et al. 1998). The Menilite shales that underlie Krosno shales in the Świątkowa Wielka tectonic window are also a very good source rock and they have generated hydrocarbons (Dziadzio and Matyasik 2004). Thermogenic hydrocarbons were generated at the maximal burial conditions, which occurred when the Magura nappe overrode the Dukla subbasin (Dziadzio and Matyasik 2004). However, hydrocarbons could have also been generated earlier by microbial methanogenesis. It probably took place during the last stages of deposition in the Dukla subbasin, when the source Menilite shales were buried below the Krosno Formation at a few hundred meters depth. The light hydrocarbons produced (mainly methane) migrated upwards and/or were incorporated into the gas hydrates at places where favorable *P–T* conditions existed. However, an additional deeper source of hydrocarbons cannot be excluded, because the $\delta^{13}C$ values of the seep carbonates are not indicative of either biogenic or thermogenic hydrocarbons as the source of carbonate carbon.

Evidence of gas hydrate occurrence

The calcite fringe cements in the druses from the examined polymictic breccia have precipitated in cavities. It is deduced not only from their fringing character, but also from the fact that they are barren of sediment particles and that some druses are still hollow in the center (Figs. 5, 6c, e, 7a). However, the druses exhibit a clast-like appearance (Figs. 5, 6) which suggests that these spaces had originally been particles composed of a solid substance. It is proposed that they had been gas hydrate aggregates.

Gas hydrate aggregates are found within active seep carbonates (Bohrmann et al. 1998; Suess et al. 1999; Pellenbarg and Max 2000). Bohrmann et al. (1998) and Suess et al. (1999) reported on authigenic carbonates associated with gas hydrates of the Cascadia margin. Gas hydrates were found filling veins, fractures and globular cavities, which were interpreted as former gas bubbles. Aragonite cement, which precipitated within the gas hydrate, outlined the globular texture of the hydrate (Bohrmann et al. 1998). Peckmann and Thiel (2004) proposed that such globular texture in ancient seep carbonates may indicate their relation with former gas hydrates. However, gas hydrate aggregates of various shapes are also detached and transported as clasts through the conduit zones in modern cold seeps (Suess et al. 2001; Milkov et al. 2004). Consequently, gas hydrate-associated carbonates may also mimic the shape of a clast, which is the proposed interpretation for the clast-like druses examined. However, it is not clear whether the gas hydrate aggregates migrated with gas-bearing fluids from deeper diagenetic zones or formed in situ and were brecciated afterwards.

The gas hydrate aggregates were cemented within the carbonate build-up by the very intensive carbonate precipi-

tation. They dissociated at some point and oxidation of the liberated methane probably induced carbonate precipitation on the cavity walls. This is supported by the very negative $\delta^{13}C$ values (as low as −30‰) of the calcite cement which fills the druses. Because the *Beggiatoa*-like filaments are rooted within the fringe cement (Fig. 7d), it is even possible that the bacteria lived directly on the surface of the decomposing gas hydrate aggregates (see Sassen et al. 2004).

Gas hydrate decomposition and methane migration

A significant drop of relative sea level that began in the Silesian basin in the Late Oligocene was related to the formation and progradation of the accretionary prism (Poprawa et al. 2002; Oszczypko 2004) and was probably responsible for gas hydrate dissociation. The resultant release of light, gas-charged waters and the fluid expulsion caused a large-scale ascent of the fluids. This migration could have contributed to regional slope destabilization in the Silesian basin by overpressurization and fluidization of shallow, poorly consolidated sediments. Large submarine slumps and soft-sediment deformations that are remarkably numerous in the Krosno Formation might have been caused by these processes (see Kennett and Fackler-Adams 2000). This scenario of hydrate-derived gas seepage caused by accretionary prism formation in convergent margin settings is analogous to the recent situation at the Cascadia margin offshore Oregon (see Ritger et al. 1987; Bohrmann et al. 1998; Suess et al. 1999; Teichert et al. 2005). The best ancient counterpart of the examined palaeoseep is found in the northern Apennines, where Miocene seep carbonates of similar lithological features were formed in an analogous geotectonic and sedimentary environment (see Conti and Fontana 1999, 2002, 2005).

Although reservoir rocks in the Outer Carpathians have been extensively examined, no hydrocarbons were found that could be correlated with the organic matter from the Menilite shales from Świątkowa Wielka (Dziadzio and Matyasik 2004). The inferred presence of gas hydrates in the basin provides a reasonable explanation for this situation. If methane generated from the Menilite shales was incorporated into hydrates, it could be emitted later into the water column (see Suess et al. 1999) due to the dissociation of gas hydrates. The cold-seep carbonates examined constitute the terminal by-product of this hydrocarbon migration, which was probably caused by subduction-induced gas hydrate decomposition in the Silesian basin.

Conclusions

The authigenic carbonates examined formed as by-products of hydrocarbon oxidation in near-surface sediments as evidenced by the low $\delta^{13}C$ values and the composition of fluid inclusions. The precipitation of carbonate gave rise to the concretions, the laminated limestone bed, and the carbonate build-up. Diffuse methane seepage induced the formation of the concretions. A more intensive methane discharge resulted in the limestone bed, which acted as a permeability barrier. The resultant overpressure in pore waters caused fluidization and soft-sediment deformations in the mudstone. The subsequent rise of fluids became structurally aligned and significantly increased the overpressure. The abrupt release of gas-charged fluids caused intensive chaotic brecciation, which occurred repeatedly and interchangeably with cementation. This recycling process gradually led to the development of the carbonate build-up with its distinctive internal structure.

Seep-related microbial activity is indirectly inferred from the mixed type of OM and the presence of calcified biofilms from the breccia. However, preservation of fossilized filaments of *Beggiatoa*-like bacteria is the direct proof of microbial activity. These filaments occur in characteristic clast-like druses, which are probably former gas hydrate aggregates. Dissociation of the gas hydrate provided substrates for microbial activity, which induced carbonate precipitation.

The evaluation of gas hydrate stability in the Silesian basin in Oligocene times showed that they could form at depths exceeding 500 m below sea level. The most evident possible source of hydrocarbons for gas hydrate precipitation is the Menilite Formation, which underlies the Krosno Formation. It is not clear whether gas hydrates were formed in situ within the carbonate build-up or were transported together with the methane-charged fluids from deeper burial settings. Nonetheless, the occurrence of gas hydrate deposits is consistent with geotectonic and palaeobathymetric data and offers a likely explanation of the major phenomena that occurred in the Silesian basin in Oligocene.

Acknowledgements This paper is a part of a Ph.D. thesis finished in 2005 at the Faculty of Geology, Warsaw University. Funding for this research was provided by the Polish Ministry of Education and Science (State Committee for Scientific Research grant no. 6 P04D 03721) and by the Institute of Geochemistry, Mineralogy and Petrology, Warsaw University. I am particularly grateful to Andrzej Barczuk for his effective scientific supervision during the research. I would also like to thank Andrzej Kozłowski for the examination of fluid inclusions, Ewa Słaby for the constructive comments on the earlier version of the manuscript and Euan Clarkson for the revision of the final version of the text. Careful and valuable reviews of the manuscript by Jörn Peckmann and an anonymous reviewer are gratefully acknowledged.

References

Barbieri R, Cavalazzi B (2005) Microbial fabrics from Neogene cold seep carbonates, Northern Apeninne, Italy. Palaeogeogr Palaeoclimatol Palaeoecol 227:143–155

Boetius A, Ravenschlag K, Schubert CJ, Rickert D, Widdel F, Gieske A, Amann R, Jørgensen BB, Witte U, Pfannkuche O (2000) A

marine microbial consortium apparently mediating anaerobic oxidation of methane. Nature 407:623–626
Bohrmann G, Greinert J, Suess E, Torres M (1998) Authigenic carbonates from the Cascadia subduction zone and their relation to gas hydrate stability. Geology 26:647–650
Bojanowski MJ (2001) Determination of growth mechanisms and burial settings of calcite concretions in the Krosno Shales (Polish Outer Carpathians) based on macro and microscopic observations. Pol Tow Mineral Prace Spec 18:15–28
Burtan J, Chowaniec J, Golonka J (1984) Preliminary results of studies on exotic carbonate rocks in the western part of the Polish flysch Carpathians (in Polish, summary in English). Biul Inst Geol 346:146–159
Campbell KA (2006) Hydrocarbon seep and hydrothermal vent paleoenvironments and paleontology: past developments and future research directions. Palaeogeogr Palaeoclimatol Palaeoecol 232:362–407
Cavagna S, Clari P, Martire L (1999) The role of bacteria in the formation of cold seep carbonates: geological evidence from Monferrato (Tertiary, NW Italy). Sediment Geol 126:253–270
Cieszkowski M, Ślączka A, Wdowiarz S (1985) New data on structure of the flysch Carpathians. Prz Geol 6:313–333
Conti S, Fontana D (1999) Miocene chemoherms of the northern Apennines, Italy. Geology 27:927–930
Conti S, Fontana D (2002) Sediment instability related to fluid venting in Miocene authigenic carbonate deposits of the northern Apennines (Italy). Int J Earth Sci 91:1030–1040
Conti S, Fontana D (2005) Anatomy of seep-carbonates: ancient examples from the Miocene of the northern Apeninnes (Italy). Palaeogeogr Palaeoclimatol Palaeoecol 227:156–175
Cranston RE, Buckley D (1990) Redox reactions and carbonate preservation in deep-sea sediments. Mar Geol 94:1–8
Dillon WP, Max MD (2000) Oceanic gas hydrate. In: Max MD (ed) Natural gas hydrate in oceanic and permafrost environments. Springer, New York, pp 61–76
Dziadzio P, Matyasik I (2004) Rekonstrukcja systemu naftowego i jego znaczenie na wybranych przykładach z jednostek dukielskiej i śląskiej (in Polish). In: LXXV Zjazd Naukowy PTG, Iwonicz Zdrój, Poland, pp 55–67
Dżułyński S, Radomski A (1956) Clastic dikes in the Carpathian Flysch. Ann Soc Geol Pol 26:225–264
Friedman GM (1959) Identification of carbonate minerals by staining methods. J Sediment Petrol 29:87–97
Jahnke RA, Craven DB, Gaillard JF (1994) The influence of organic matter diagenesis on $CaCO_3$ dissolution at the deep-sea floor. Geochim Cosmochim Acta 58:2799–2809
Jørgensen BB, Gallardo VA (1999) *Thioploca* spp.: filamentous sulfur bacteria with nitrate vacuoles. FEMS Microbiol Ecol 28:301–313
Jørgensen BB, Revsbech NP (1983) Colorless sulfur bacteria, *Beggiatoa* spp. and *Thiovulum* spp., in O_2 and H_2S microgradients. Appl Environ Microbiol 45:1261–1270
Joye SB, Boetius A, Orcutt BN, Montoya JP, Schultz HN, Erickson MJ, Lugo SK (2004) The anaerobic oxidation of methane and sulfate reduction in sediments from Gulf of Mexico cold seeps. Chem Geol 205:219–238
Jucha S, Kotlarczyk J (1961) Seria menilitowo-krośnieńska w Karpatach fliszowych (in Polish). Pr Geol PAN 4:1–115
Kennett JP, Fackler-Adams BN (2000) Relationship of clathrate instability to sediment deformation in the upper Neogene of California. Geology 28:215–218
Köster J, Kotarba M, Lafargue E, Kosakowski P (1998) Source rock habitat and hydrocarbon potential of Oligocene Menilite Formation (Flysch Carpathians, Southeast Poland): an organic geochemical and isotope approach. Org Geochem 29:543–558
Koszarski L (1985) Geology of the middle Carpathians and the Carpathian Foredeep. In: Guide to excursion 3, Carpatho-Balkan Geological Association XIII Congress, Cracow, Poland
Kozikowski H (1956) Ropa-Pisarzowa unit: a new tectonic unit of the Polish flysch Carpathians (in Polish, summary in English). Biul Inst Geol 110:93–137
Książkiewicz M (1949) Slip-bedding in the Carpathian Flysch (in Polish, summary in English). Ann Soc Geol Pol 19:493–504
Książkiewicz M (1958) Submarine slumping in the Carpathian Flysch. Ann Soc Geol Pol 28:123–151
Książkiewicz M (1975) Bathymetry of the Carpathian Flysch basin. Acta Geol Pol 25:309–367
Książkiewicz M (1977) Hypothesis of plate tectonics and the origin of the Carpathians. Ann Soc Geol Pol 47:329–353
Larkin JM, Henk MC (1989) Is "hollowness" an adaptation of large prokaryotes to their largeness? Microbios Lett 42:69–72
Larkin J, Aharon P, Henk MC (1994) *Beggiatoa* in microbial mats at hydrocarbon vents in the Gulf of Mexico and Warm Mineral Springs, Florida. Geo Mar Lett 14:97–103
Mastella L, Rubinkiewicz J (1998) Duplex structures within the Świątkowa Wielka tectonic window (Beskid Niski Mts., Western Carpathians, Poland): structural analysis and photointerpretation. Geol Q 42:173–182
Milkov AV, Vogt PR, Crane K, Lein AY, Sassen R, Cherkashev GA (2004) Geological, geochemical, and microbial processes at the hydrate-bearing Håkon Mosby volcano: a review. Chem Geol 205:347–366
Mochnacka K, Tokarski A (1972) A new occurrence of exotic blocks in the Krosno Beds near Ustrzyki Górne (Bieszczady Range, Polish Eastern Carpathians) (in Polish, summary in English). Ann Soc Geol Pol 42:229–238
Nelson DC, Wirsen CO, Jannasch HW (1989) Characterization of large, autotrophic *Beggiatoa* spp. abundant at hydrothermal vents of the Guaymas basin. Appl Environ Microbiol 55:2909–2917
Nemčok M, Nemčok J, Wojtaszek M, Ludhova L, Oszczypko N, Sercombe WJ, Cieszkowski M, Paul MP, Coward MP, Ślączka A (2001) Reconstruction of Cretaceous rifts incorporated in the Outer West Carpathian wedge by balancing. Mar Pet Geol 18:39–64
Olszewska B (1984) Interpretacja paleoekologiczna otwornic kredy i paleogenu polskich Karpat zewnętrznych (in Polish). Biul Inst Geol 346:7–45
Orphan VJ, House CH, Hinrichs K-U, McKeegan KD, DeLong EF (2001) Methane-consuming archea revealed by direct coupled isotopic and phylogenetic analysis. Science 293:484–487
Oszczypko N (2004) The structural position and tectonosedimentary evolution of the Polish Outer Carpathians. Prz Geol 52:780–791
Oszczypko-Clowes M, Oszczypko N (2004) The position and age of the youngest deposits in the Mszana Dolna and Szczawa tectonic windows (Magura Nappe, Western Carpathians, Poland). Acta Geol Pol 54:339–367
Peckmann J, Thiel V (2004) Carbon cycling at ancient methane-seeps. Chem Geol 205:443–467
Peckmann J, Thiel V, Michaelis W, Clari P, Gaillard C, Martire L, Reitner J (1999) Cold seep deposits of Beauvoisin (Oxfordian; southeastern France) and Marmorito (Miocene; northern Italy): microbially induced authigenic carbonates. Int J Earth Sci 88:60–75
Peckmann J, Thiel V, Reitner J, Taviani M, Aharon P, Michaelis W (2004) A microbial mat of a large sulfur bacterium preserved in a Miocene methane-seep limestone. Geomicrobiol J 21:247–255
Pellenbarg RE, Max MD (2000) Introduction, physical properties, and natural occurrences of hydrate. In: Max MD (ed) Natural gas hydrate in oceanic and permafrost environments. Springer, New York, pp 1–8

Pescatore T, Ślączka A (1984) Evolution models of two flysch basins: the northern Carpathians and the southern Apennines. Tectonophysics 106:49–70

Picha FJ, Stranik Z (1999) Late Cretaceous to early Miocene deposits of the Carpathian foreland basin in southern Moravia. Int J Earth Sci 88:475–495

Poprawa P, Malata T, Oszczypko N (2002) Tectonic evolution of the Polish part of Outer Carpathian's sedimentary basins: constraints from subsidence analysis (in Polish, summary in English). Prz Geol 50:1092–1108

Riding R (2002) Biofilm architecture of Phanerozoic cryptic carbonate marine veneers. Geology 30:31–34

Ritger S, Carson B, Suess E (1987) Methane-derived authigenic carbonates formed by subduction-induced pore-water expulsion along the Oregon/Washington margin. Geol Soc Am Bull 98:147–156

Roedder E (1984) Fluid inclusions. Rev Mineral 12. Mineralogical Society of America, Chantilly, VA, USA, 644 pp

Sakai H, Gamo T, Ogawa Y, Boulegue J (1992) Stable isotopic rations and origins of the carbonates associated with cold seepage at the eastern Nankai Trough. Earth Planet Sci Lett 109:391–404

Sassen R, Roberts HH, Aharon P, Larkin J, Chinn EW, Carney R (1993) Chemosynthetic bacterial mats at cold hydrocarbon seeps: Gulf of Mexico continental slope. Org Geochem 20:77–89

Sassen R, Roberts HH, Carney R, Milkov AV, DeFreitas DA, Lanoil B, Zhang C (2004) Free hydrocarbon gas, gas hydrate, and authigenic minerals in chemosynthetic communities of the northern Gulf of Mexico continental slope: relation to microbial processes. Chem Geol 205:195–217

Suess E, Torres ME, Bohrmann G, Collier RW, Greinert J, Linke P, Rehder G, Trehu A, Wallmann K, Winckler G, Zuleger E (1999) Gas hydrate destabilization: enhanced dewatering, benthic material turnover and large methane plumes at the Cascadia convergent margin. Earth Planet Sci Lett 170:1–15

Suess E, Torres ME, Bohrmann G, Collier RW, Rickert D, Goldfinger C, Linke P, Heuser A, Sahling H, Heeschen K, Jung C, Nakamura K, Greinert J, Pfannkuche O, Trehu A, Klinkhammer G, Whiticar MJ, Eisenhauer A, Teichert B, Elvert M (2001) Sea floor methane hydrates at Hydrate Ridge, Cascadia Margin. In: Paull CK, Dillon WP (eds) Natural gas hydrates: occurrence, distribution and detection. Am Geophys Union Geophys Monogr 124:87–98

Ślączka A (1961) Exotic-bearing shale from Bukowiec (Polish Eastern Carpathians) (in Polish, summary in English). Ann Soc Geol Pol 31:129–143

Ślączka A, Wieser T (1962) Shales with exotics in the Krosno Beds of the Baligród region (Polish Eastern Carpathians) (in Polish, summary in English). Geol Q 6:662–678

Teichert BMA, Bohrmann G, Suess E (2005) Chemoherms on Hydrate Ridge: unique microbially-mediated carbonate build-ups growing into the water column. Palaeogeogr Palaeoclimatol Palaeoecol 227:67–85

Unrug R (1968) Kordyliera Śląska jako obszar źródłowy materiału klastycznego piaskowców fliszowych Beskidu Śląskiego i Beskidu Wysokiego (Polskie Karpaty zachodnie) (in Polish). Ann Soc Geol Pol 38:81–164

Van Couvering JA, Aubry MP, Berggren WA, Bujak JP, Naeser CW, Weiser T (1981) The terminal Eocene event and the Polish connection. Palaeogeogr Palaeoclimatol Palaeoecol 36:321–362

Von Rad U, Rösch H, Berner U, Geyh M, Marchig V, Schulz H (1996) Authigenic carbonates derived from oxidized methane vented from the Makran accretionary prism off Pakistan. Mar Geol 136:55–77

Wachter E, Hayes JM (1985) Exchange of oxygen isotopes in carbon dioxide–phosphoric acid systems. Chem Geol 52:365–374

Wellsbury P, Parkes RJ (2000) Deep biosphere: Source of methane for oceanic hydrate. In: Max MD (ed) Natural gas hydrate in oceanic and permafrost environments. Springer, New York, pp 91–104

Whiticar MJ, Faber E (1986) Methane oxidation in sediment and water column environments: isotope evidence. Org Geochem 10:759–768